

# VIEW DIRECTIONS OF THE NARROW FOV SENSORS FOR BARE SOIL/ROCK ALBEDO EVALUATION WITH MINIMAL ERRORS

J. Cierniewski<sup>a</sup>, T. Gdala<sup>b</sup>

<sup>a</sup> Department of Soil Science and Remote Sensing of Soils, Institute of Physical Geography and Environmental Planning, Adam Mickiewicz University, Dziejelowa 27, 61-680 Poznan, Poland - ciernje@amu.edu.pl

<sup>b</sup> Mathematics and Computer Science Faculty, Adam Mickiewicz University, Umultowska 87, 61-614 Poznan, Poland - tgdala@amu.edu.pl

**KEY WORDS:** Soil, Modelling, Error, Radiation, Sensor, Optical

## ABSTRACT:

This paper discusses the errors resulting from evaluation of the spectral albedo of smooth and rough bare soil or rocky surfaces by one view of the narrow FOV sensor under clear sky conditions in the optical domain for specified, whole days from sunrise to sunset: 22<sup>nd</sup> December, 5<sup>th</sup> February, 21<sup>st</sup> March, 6<sup>th</sup> May, 22<sup>nd</sup> June, 6<sup>th</sup> August, 23<sup>rd</sup> September and 5<sup>th</sup> November. It was assumed that these surfaces were located at one time in Israel near Beer Sheva (31.3°N, 34.7°E), than in France near Saint Remy (43.7°N, 4.9°E) and in Poland near Poznań (52.0°N, 16.9°E). The paper considers from which directions the sensor should collect the reflectance data of these surfaces to treat them as describing their spectral albedo with minimal error. The hemispherical-directional model, earlier used to explain image distinction between cultivated and uncultivated bare surfaces (Cierniewski *et al.*, 2004), was applied to accomplish the goal of this paper. Results of the analysis show that the spectral albedo of the analysed surfaces for periods longer than a day should be measured along the North–South direction. The surface albedo for summer period should be described by the reflectance measurement taken from higher zenith angles than for winter period. The errors, describing this means of albedo measurement, calculated as the values dependent on the reflected energy level, reach their maximum, 3–4%, at the beginning of spring and autumn, while their minimum, lower than 2%, at the beginning of summer and winter.

## INTRODUCTIONS

Irregularities of bare soil or rocky surfaces, caused by their texture, aggregates and microrelief configuration, that are large when compared with wavelengths in the optical domain and are opaque, cast shadows on these surfaces. Shaded soil fragments reflect many orders-of-magnitude less energy than the sunlit ones. Variation of the shadow area in relation to the sunlit one is a basic reason of the surfaces non-equal reflection in all directions. The reflectance of the soil or rocky surfaces varies due to the directions of its illumination and observation. Cultivated soil surfaces, with dominant diffuse features, reflect less light if direct beams, like a solar, come to the surfaces more obliquely. They usually reflect more light from backscattering directions near the zenith and azimuth position of the sun, which makes the lowest proportion of their shaded fragments. However, these surfaces reflect less the energy from the extreme forwardscatter direction near the horizon, from which the highest fraction of their shaded parts is visible. Milton and Webb (1987), examining the influence of cultivation practices on the direct reflectance of sandy soils, observed that ploughing considerably decreased soil reflectance. They also found that the peak of backscatter radiation became less pronounced at a low solar zenith angle. Weak symptoms of a forwardscattering character of the reflectance of cultivated bare soils were noticed by Irons and Smith (1990). They reported that the roughest ploughed soil surface of a fine-loamy texture, scattered radiation forward as strongly as the smoothest surface. The relatively larger shadowing of the roughest soil in compensation for its strong forwardscatter was given as the reason of the effect. Coulson (1966) found that desert soil materials like gypsum sand and beach quartz sand display a high reflectance with a strong forwardscatter maximum for the visible and near-infrared range. The directional reflectance of these soil surfaces clearly vary with the angle of the incident radiation. Shoshany

(1993), analysing directional reflectance data sets of desert stony pavements and rocky surfaces in Australia, found that most of the surfaces exhibited an anisotropic reflection with clear backscattering component. The backscatter, as well as the forwardscatter, regimes in soil reflectance have been noticed by Deering *et al.* (1990). They have demonstrated it on the examples of an alkali flat bare soil and dune sand surface.

The non-equal reflectance distribution from the soil or rocky surfaces, becoming clear for higher solar zenith angles and higher atmosphere transparency, is also caused by a more non-equal distribution of sky energy in illumination conditions varying in this way. The angular distribution of sky radiation for a clear and clean shows that the sky is very bright near the sun in the so-called aureole (Fraser, 1975). The sky is a relatively bright along the horizon, while it is the darkest in the quadrant opposite to the sun. The variation of the sky radiance intensity becomes lower when sun elevation raises. Kondratyev (1969) has mentioned that the variation could be practically negligible for sun elevation angles higher than 60°. The amount of the diffuse light in the global skylight coming to the earth's surfaces varies with cloudiness. When the sky is completely overcast, the radiance distribution is almost even with its weak monotonic drop from the zenith to the horizon.

The two hemispherical radiation environments, one incoming and one outgoing, can be described by the bidirectional reflectance distribution function *BRDF*. The *BRDF* is described as the ratio of the radiance reflected by the surface to the incident irradiance from a single source of illumination. Similarly, the bidirectional reflectance factor *BRF* is defined with a single source of the incident radiation only. It is described as the radiance reflected by the surface to the radiance which would be reflected by a perfect Lambertian panel, both under the same illumination and viewing conditions (Milton, 1989). In field conditions, the limitation of only one the direct solar source of radiation would mean the elimination of the

diffuse sky radiation. Because it is unreal, for reducing the sky radiation influence, the directional reflectance measurements, taken on a day with a clear sky, under thin and stable aerosol conditions, for wavelengths for which the sky radiance can be neglected, are recommended (Sandmeier, 2000). Sets of the directional reflectance measurements, related to a specific distribution of the sun and the sky irradiation, cannot be combined with the other sets taken at different atmospheric conditions. When the incident radiance measured in field condition includes direct solar radiation as well as diffuse skylight, the bidirectional reflectance factor *BRF*, should be called the hemispherical-directional reflectance factor *HDRF* (Engelson, *et al.*, 1996). Abdou *et al.* (2001) and Strub *et al.* (2003) suggest that the practical data about the directional reflectance behaviour of different objects that have been collected so far, require the use of the hemispherical-directional reflectance factor, rather than the bidirectional reflectance approach, because the incident irradiance consist of a mixture of direct solar and non-isotropic diffuse illumination.

The albedo, widely used in studies on energy transfer between soil, vegetation and atmosphere, as well as on climate studies at global and regional scales, is the bihemispherical factor. This quantity, as a dimensionless term, expresses the ratio of the total short-wave (0.3-3  $\mu\text{m}$ ) radiant exitance of reflected energy by a surface in all directions to the total downwelling irradiance. The albedo characterizing the intrinsic properties of a given surface also depends on its illumination conditions, position of the sun and the atmosphere state, i.e., cloudiness and contents of aerosols and their quality. The non-equal spectral reflectance distribution of natural land surfaces, like the soil or rocky, makes the albedo measurements by satellite radiometers difficult. Although this technology supplies spatially variable and temporally dynamic data, satellite sensors mostly sense the radiance of given earth surfaces at one or only a few directions, inside their small field of view and relatively narrow spectral ranges. Therefore, special models have been used for recovering the albedo parameter from the satellite data.

Being aware that the non-equal distribution of the short-wave energy reflected in all directions from land surfaces dynamically varies during a day, depending on the solar zenith angle and the atmosphere state, the authors of this paper consider from which directions the narrow FOV sensor should look at bare soil or rocky surfaces, located at three different latitudes to treat the reflected signal from the surfaces as describing their albedo for specified whole days from sunrise to sunset with the minimal errors. These errors are discussed on the examples of the hemispherical-directional data of two surfaces, generated by the model earlier used for explanation image distinction between cultivated and uncultivated bare surfaces (Cierniewski *et al.*, 2004).

## METHODS

### The model

This model simulates a soil or rocky surface as a geometrical creation similar to beads merging into each other. This virtual surface is characterized by three parameters *a*, *b* and *c*. The *a* and *b* describe its height variation along the *x*-axis and the *y*-axis, by the amplitude of the sinus function. The *c* expresses the disturbance in the height position in relation to that determined by only the *a* and *b* parameters. The virtual surface, as an opaque object, is illuminated by a hemispherical light source created by a number of point sources of given light intensities, equally spread on the hemisphere. It is assumed that for outdoor conditions the ratio of the direct solar irradiance to

the global irradiance for clear sky conditions changes with the sun's position *s*, described by the solar zenith  $\theta_s$  and azimuth  $\phi_s$  angles, and the optical thickness of the atmosphere  $\tau$  attributed to the wavelength  $\lambda$ . Distribution of the hemispherical light energy is described by the formula, taking also into account: the minimum amount of the energy, the amplification of the energy near the horizon, the concentration of the solar aureole and the energy at the darkest part of the hemisphere light in the quadrant opposite the sun. All these quantities are expressed by the constants, similarly as in the equation of Grant *et al.* (1996). The light energy is scattered from the surface, in accordance the quasi-Lambertian function, being a combination of the Lambertian scattering and the quasi-specular one. The distribution of the surface hemispherical-directional reflectance *HDR*(*s*, $\tau$ ,*v*) as viewed from all the possible directions *v*, defined by the zenith  $\theta_v$  and azimuth  $\phi_v$  angles, can be generated for all the possible illumination conditions *s* expressed by the angles  $\theta_s$ ,  $\phi_s$  and the atmosphere optical thickness  $\tau$ , attributed to the given wavelength  $\lambda$ .

### Conditions of the albedo evaluation and errors resulting from it

In this paper our attention is focused on the soil/rock *HDR*, normalized, *NHDR*, in this way that independently on illumination conditions its average value is equal to 1, i.e.:

$$NHDR(s, \tau, v) = \frac{HDR(s, \tau, v)}{\int_v HDR(s, \tau, v) dV}. \quad (1)$$

The function  $\bar{H}(s, \tau, v)$ , expressing the deviation from the *NHDR*(*s*, $\tau$ ,*v*) average value, can be given as:

$$\bar{H}(s, \tau, v) = |1 - NHDR(s, \tau, v)|. \quad (2)$$

To accomplish the paper goals, the relative albedo error  $\bar{\alpha}_{p,d}$ , expressed as:

$$\bar{\alpha}_{p,d} = \min_v \max_{s \in S_{p,d}} \bar{H}(s, v), \quad (3)$$

and the view directions  $V_{p,d}$  for which  $\bar{\alpha}_{p,d}$  it is accessible, given as:

$$V_{p,d} = \left\{ v : \max_{s \in S_{p,d}} \bar{H}(s, v) = \bar{\alpha}_{p,d} \right\} \quad (4)$$

were calculated for the illumination data sets  $S_{p,d}$ . The sets relate to all the sun positions in clear sky conditions for a specified day *d* at a given place of Earth *p*, described by its geographical coordinates.

Two virtual surfaces, a relatively rough one and a smooth one, of their clearly different directional reflectance distribution, were used to reach these objectives.

## RESULTS

### The studied surfaces and their virtual equivalents

These surfaces were chosen as equivalents of real soil and rocky surfaces, located in Israel, cultivated with soil aggregates randomly dispersed and the smooth desert (Fig. 1). This first one represents *Calcic Xerosol*, developed from sandy loam with 0.6% of organic matter content and 16% of  $\text{CaCO}_3$  content in the surface horizon. The soil is located near Beer-Sheva (31.33°N, 34.67°E) in a field prepared by a rotary harrow. The second one characterizes the silty surface near Sede Boker (30.84°N, 34.78°E) in the Negev desert. The cultivated and the uncultivated surfaces, with their height irregularities randomly dispersed, are simulated by virtual surfaces with  $b=1$ . Virtual surfaces simulating cultivated surfaces with a furrow microrelief having clearly directional shape, expressed by the parameter  $0 < b < 1$ . The greater the roughness of the real surfaces, the greater that of their virtual equivalents, expressed by their relatively high parameters  $a$  and  $c$ . The virtual surface of the relatively smooth surface (SB) is described by  $a=0$ , deformed only by the disturbance parameter  $c=0.3$ .

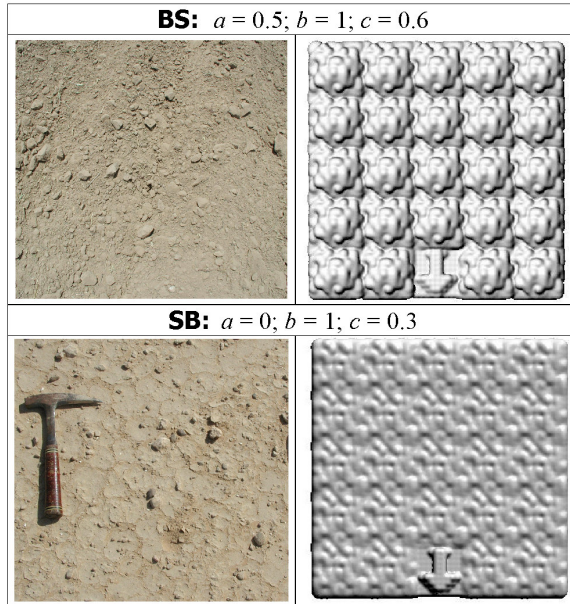


Figure 1. View of the studied surfaces and their virtual equivalents: the desert smooth (SB) and the cultivated rough (BS). The symbols  $a$ ,  $b$  and  $c$  are geometrical parameters of the virtual surfaces. The arrow shows the North direction

### Directional reflectance of the studied surfaces

These virtual surfaces were used as the input data sets to predict the hemispherical-directional reflectance *HDR* of the analysed surfaces in clear sky conditions for the following values of the optical atmosphere thickness  $\tau$ : 0.15, 0.2, 0.35, 0.4 and 0.5, attributed with the wavelengths  $\lambda$ : 1650 nm, 850 nm, 650 nm, 550 nm and 450 nm, respectively. Their *HDR* distributions were generated for all possible view directions,

described by the zenith angle  $\theta_v$ , at a wide range of the solar zenith angle  $\theta_s$  between 10° and 80°. The examples of the *HDR* distributions, normalized to the nadir viewing, presented in Fig. 2, show them only for the  $\theta_s$  20°, 40°, 60°, and 80° and the  $\tau$  0.2 corresponding to the wavelength of 850 nm. Variation of the  $\theta_v$  is marked by concentric circle lines surrounding the nadir point ( $\theta_v=0^\circ$ ) at 10° increments spread on the top of the graphs. These distributions are positioned with respect to the geographical North direction (N) marked at their bottom.

The cultivated rough surface (BS) demonstrates a clearly higher variation of its *HDR*, than the desert smooth one (SB). This relationship becomes stronger at the higher  $\theta_s$ . Both the analysed *HDR* data exhibit a backscattering character, although the ones characterizing the smooth surface (SB) at high  $\theta_s$  angles also demonstrate specular features.

### Conditions of the albedo achieving and errors resulting from it

The spectral albedo  $\alpha$  of these surfaces in clear sky conditions for the wavelengths mentioned above was calculated from their *HDR* and sky radiance data as the bispherical factor. The  $\alpha$  of the surfaces in the functions of the optical atmosphere thickness between 0.1 and 0.5, attributed with the wavelength range of about 2000 nm and 450 nm are presented in Fig. 3.

To obtain the paper goals, the  $\alpha$  of the surfaces was analysed in the illumination data sets  $S_{p,d}$ . These sets relate to all the sun positions  $p$ , from sunrise to sunset at 5° increments of the solar zenith angle  $\theta_s$ , for the specified days: 22<sup>nd</sup> December, 5<sup>th</sup> February, 21<sup>st</sup> March, 6<sup>th</sup> May, 22<sup>nd</sup> June, 6<sup>th</sup> August, 23<sup>rd</sup> September and 5<sup>th</sup> November, assuming that during these days each of the surfaces was located  $p$  at one time in Israel near Beer-Sheva (31.3°N, 34.7°E), than in France near Saint Remy (43.7°N, 4.9°E) and in Poland near Poznań (52.0°N, 16.9°E).

Results of the analysis show that the spectral albedo  $\alpha$  of both studied surfaces for periods longer than a day should be achieved by one view of the narrow FOV sensor along the North-South direction, oriented azimuthally at 0° (+) and 180° (-). In whole analysed spectrum, from 450 nm to 1650 nm, significant differences in the  $\alpha$  evaluation, as well as the directions from this parameter that should be evaluated, were not found (Fig. 4). The  $\alpha$  of the surfaces for summer period should be measured with higher zenith angles  $\theta_v$  than for winter. It was discovered that in summer the lower the latitude, the higher the  $\theta_v$  for which the  $\alpha$  can be evaluated with the minimal error  $\bar{\alpha}$ . The surfaces located in Israel should be viewed at the zenith angle  $\theta_v$  of about +65°..+70° for smooth surfaces with weak specular effects and about  $\theta_v$  +25°..+35° for rough ones. In the same period in France the smooth surfaces should be observed at the  $\theta_v$  +60°..+65° and the rough one at the  $\theta_v$  +20°..+25°, and in Poland at the  $\theta_v$  +55°..+60° and +15°..+20°, respectively. However, in winter this optimal sensor zenith position  $\theta_v$  for the smooth surfaces was determined as -50°..-45° if they are located in Israel, and as -45°..-40° and -40°..-35° if they are situated in France and Poland, respectively. In this period, the best sensor position for the rough surfaces was determined as -10°..-5°, independently on the surfaces location. The errors  $\bar{\alpha}$ , describing this means of the albedo measurement, calculated as the values dependent of the reflected energy level, reach their maximum, 3-4%, at the beginning of spring and autumn, while their minimum, lower than 2%, at the beginning of summer and winter.

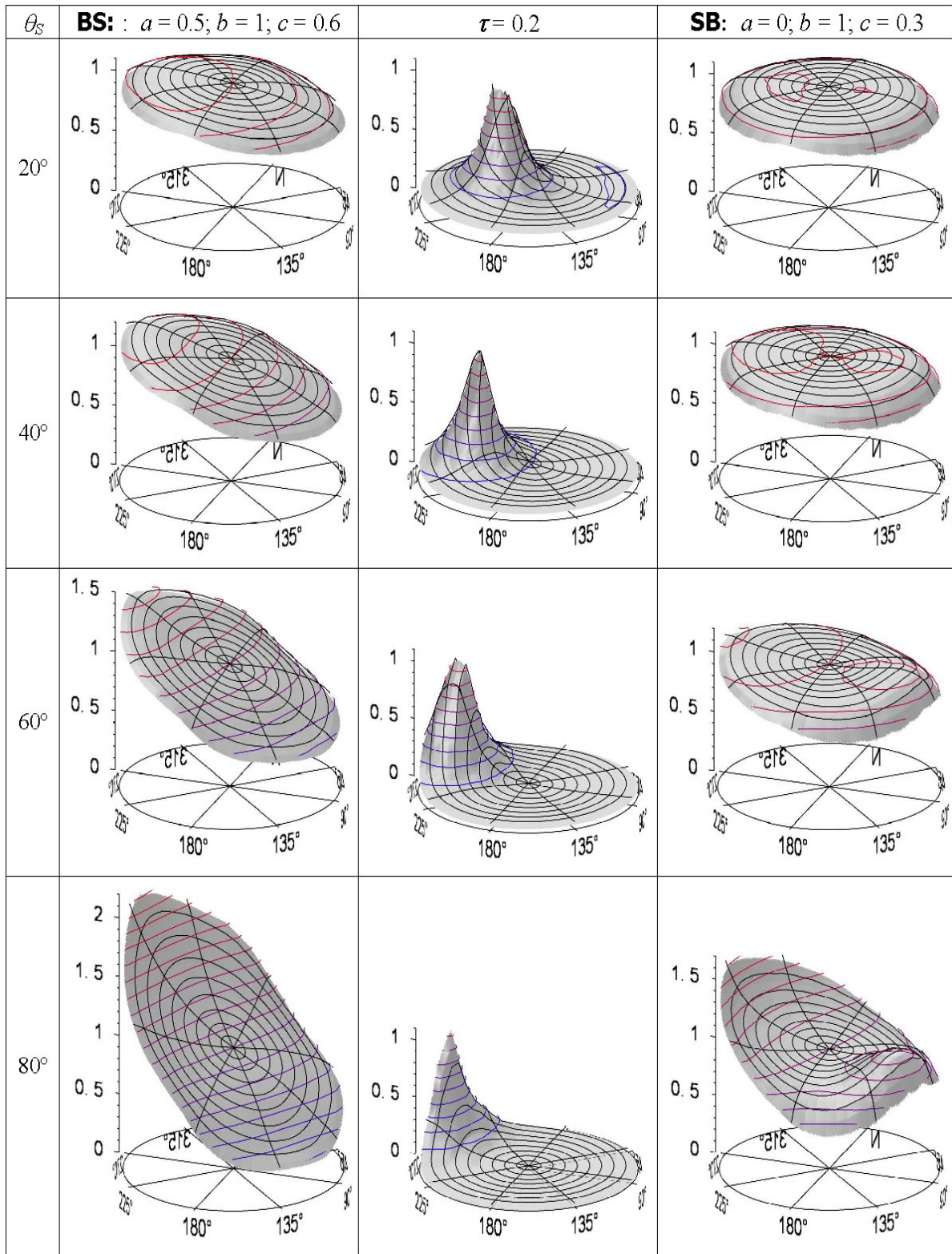


Fig. 2. Distributions of the hemispherical-directional reflectance of the desert smooth surface (SB) and the cultivated rough one (BS), normalised to the nadir viewing, generated for chosen solar zenith angle  $\theta_s$  in clear sky conditions for the wavelength of 850 nm. The sky radiation distributions connected with the selected illumination conditions, normalized to its maximum values, are presented in the middle column. The symbols  $a$ ,  $b$  and  $c$  are the geometrical parameters of the virtual surfaces

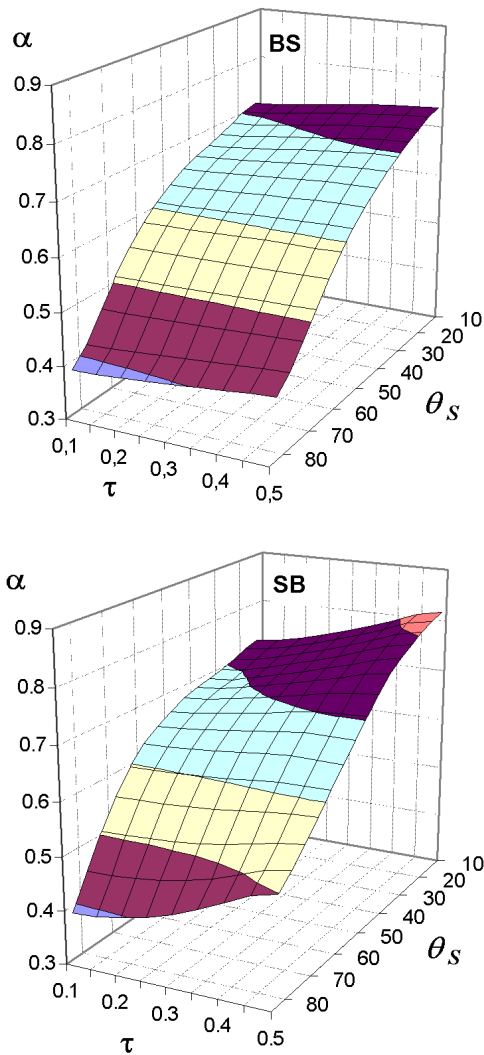


Figure 3. Distributions of the albedo for the cultivated rough surface (BS) and the desert smooth one (SB) and in clear sky conditions in the function of the solar zenith angle  $\theta_s$  and the optical thickness of the atmosphere  $\tau$

### CONCLUDING REMARKS

The results of the studies show the influence of bare soil or rocky surfaces shape and their illumination on their spectral albedo. The high sensitivity of this parameter to the surface illumination conditions, calculated as a bispherical factor, enables us to consider how the spectral albedo of the studied surfaces in diurnal periods changes with seasons, taking also into account their different location on the Earth. The results presented in this paper suggest that the evaluation of the spectral albedo of the bare surfaces by only one view of the narrow FOV sensor is available with relatively low errors.

These low errors invite us to further studies on the new way of achieving bare surfaces spectral albedo. These studies should be carried out at a higher number of days in a year, using a higher number of soil or rocky surfaces with their larger roughness variation, located in a higher number of places on the Earth, described in a wider range of their latitude.

### REFERENCES

- Abdou, W. A., Conel, J. E., Pilorz, S. H., Helmlinger, M. C., Brugge, C. J., Gaitley, B. J., Ledoboer, W. C., Martonchik, J. V., 2001. Vicarious calibration. a reflectance-based experiment with AirMISR. *Remote Sens. Environ.*, 77, pp. 338-353.
- Cierniewski J., Gdala T., Karnieli A., 2004. A hemispherical-directional reflectance model as a tool for understanding image distinctions between cultivated and uncultivated bare surfaces. *Remote Sens. Environ.*, 90, pp. 505-523.
- Coulson, K. L., 1966. Effect of reflection properties of natural surfaces in aerial reconnaissance. *Appl. Opt.*, 5, pp. 905-917.
- Deering, D. W., Eck, T. F., Otterman, J., 1990. Bidirectional reflectance of selected desert surfaces and their three-parameter soil characterization. *Agric. Forest Meteorol.*, 52, pp. 71-90.
- Engelsen, O., Pinty, B., Verstraete, M. M., Martonchik, J. V., 1996. *Parametric bidirectional reflectance factor models: evaluation, improvements and applications*. Catalogue CL-NA-16426-EN-C, ECSC-EC-EAEC Brussels, Luxembourg, p.114.
- Fraser R. S., 1975. Interaction mechanisms – within the atmosphere. In: *Manual of Remote Sensing*, American Society of Photogrammetry, Falls Church, VA, pp. 181-233.
- Grant R. H., Gao W. and Heisler G. M., 1996. Photosynthetically-active radiation: sky radiance distributions under clear and overcast conditions. *Agric. Forest Meteorol.*, 82, pp. 267-292.
- Irons, J. R., Smith, J. A., 1990. Soil surface roughness characterization from light scattering observations. *10<sup>th</sup> Annual International Geosciences and Remote Sensing Symposium*, II, pp. 1007-1010.
- Kondratyev, K., 1969. *Radiacionnyje charakteristiki atmosfery i zemnoj powerchnosti*. Gidrometeorologiceskoye Izdatelstwo. Leningrad.
- Milton, E. J., Webb, J., P., 1987. Ground radiometry and airborne multispectral survey of bare soils. *Int. J. of Remote Sens.*, 18, pp. 3-14.
- Milton, E. J., 1989. Principles of field spectroscopy. *Remote Sensing Yearbook*. 1988-1989, pp. 79-99.
- Sandmeier, S. R., 2000. Acquisition of bi-directional reflectance factor data with field goniometer. *Remote Sens. Environ.*, 73, pp. 257-269.
- Shoshany, M., 1993. Roughness-reflectance relationship of bare desert terrain: An Empirical study. *Remote Sens. Environ.*, 45, pp. 15-27.
- Strub, G., Schaepman, M. E., Knyazikhin, Y. and Itten K. I., 2003. Evaluation of Spectrodirectional alfalfa canopy data acquired during DAISEX'99. *IEEE Trans. Geosci. Remote Sens.*, 41, pp. 1034-1042.

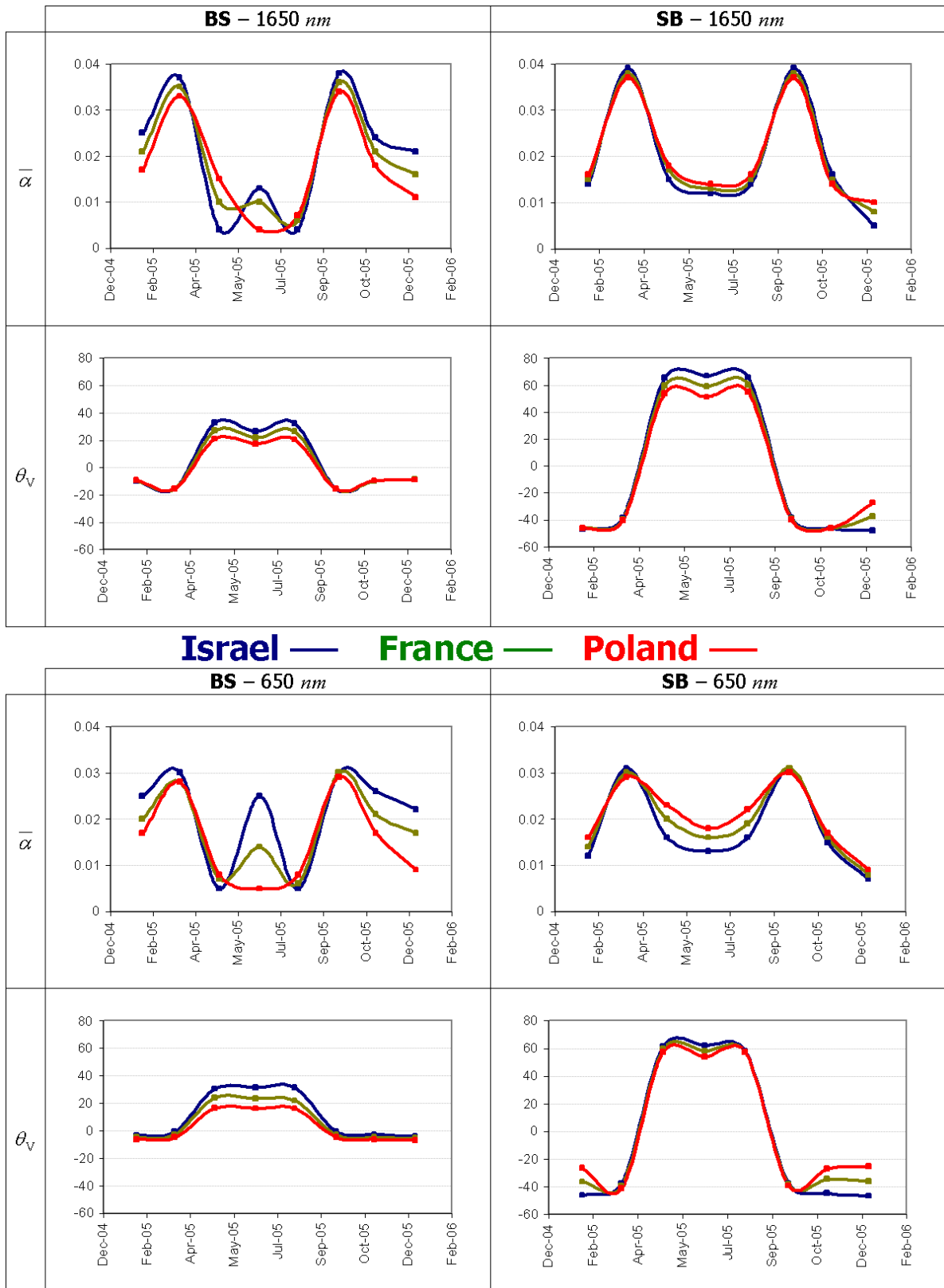


Fig. 4. Minimal errors  $\bar{\alpha}$  resulting from evaluation of the spectral albedo of the cultivated rough surface (BS) and the desert smooth one (SB) by one view of the narrow FOV sensor at its given view zenith angles  $\theta_v$  for specified days under clear sky conditions for the wavelength of 1650 nm and 650 nm